Experimental and simulation study of the high pressure oxidation of dimethyl carbonate

Katiuska Alexandrino[a,b]*, Ángela Millera[b], Rafael Bilbao[b], María U. Alzueta[b]

[a] Grupo de Biodiversidad Medio Ambiente y Salud (BIOMAS), Universidad de Las Américas, calle José Queri y Av. de los Granados / Bloque 7, Quito – EC 170125 Ecuador

[b] Aragón Institute of Engineering Research (I3A). Department of Chemical and Environmental Engineering. University of Zaragoza. C/ Mariano Esquillor, s/n. 50018 Zaragoza. Spain

Corresponding author:

Katiuska Alexandrino: katiuska.alexandrino@udla.edu.ec

+593 23981000. Extension: 7830

Abstract

An experimental and modeling study of the oxidation at high pressure of dimethyl carbonate (DMC) has been performed in a quartz tubular flow reactor. Experimental and simulated concentrations of DMC, CO, CO_2 and H_2 have been obtained for different temperatures (500-1073 K), pressures (20, 40, and 60 atm) and stoichiometries (λ = 0.7, 1, and 35). .Both pressure and concentration of oxygen are important parameters for conversion of DMC. The simulations have been carried out using a detailed kinetic mechanism previously developed by the research group. In general, the model is able to reproduce the experimental trends of the different concentration profiles, although some discrepancies are observed between experimental and simulation results. The performance of the model was also evaluated through the simulation of literature data of the oxidation of DMC at atmospheric pressure in a flow reactor and of the DMC ignition delay times under low and high pressures. In this sense, this work contributes to the knowledge of the combustion process of DMC, by providing new experimental data on the conversion of DMC at high pressures and using a kinetic model for the interpretation of the results.

Keywords: Experimental, modeling, pressure, flow reactor, kinetics

Introduction

Diesel engines are known to emit large amounts of particulate matter (PM) into the atmosphere due to the fuel composition and the non homogeneous mixing, which favours its formation in the fuel-rich regions of the chamber where the temperature is high. In this sense, the addition of oxygenated compounds to diesel fuel has been recognized to reduce PM emissions [1-5]. The use of these additives modifies some fuel properties, such as volatility, cetane index, enthalpy of combustion, etc., which, depending on the operating conditions, affect the fuel consumption and emissions. Moreover, the increase of the amount of oxygen content in the blend with diesel improves the combustion process. Biodiesel is a common oxygenated compound used in diesel engines. Bioethanol, the biofuel widely used as a gasoline alternative [6], can also be added to diesel fuel in a small percentage [7-10]. However, these oxygenated biofuels suffer from issues, such as high production cost [11], that lead to the search for improved alternatives.

In this line, the carbonate ester dimethyl carbonate (DMC, $CH_3OCOOCH_3$) is highlighted as a potential additive for diesel fuel, due to its physicochemical characteristics, such as high oxygen content (53.3 wt%), low boiling point, high miscibility with diesel fuel and its insolubility in water [12-14]. Furthermore, the absence of C-C chemical bonds contributes to the hydrocarbon oxidation rather than its participation in soot growth reactions [15]. Works performed on the addition of DMC to diesel fuel [16-20] and in flames of diesel fuel surrogates [21,22] have shown its capacity to reduce soot formation. Moreover, DMC could be directly produced from the reaction of methanol with CO_2 by catalytic procedures, making the DMC production a CO_2 sink, and, thus, contributing to the reduction of this greenhouse gas [23-25]. However, special precautions for fuel storage and distribution are needed due to the high volatility of DMC compared to diesel fuel [26].

In order to contribute to interpret and understand the reaction schemes that occur during the combustion process and, thus, to have information on the mechanisms responsible for reducing PM emissions, the investigations on DMC conversion have been focused on performing experiments in laboratory conditions, together with kinetic studies. Different studies addressing the thermal decomposition and photolysis of DMC are reported in literature [27-30], as well as works on opposed flow diffusion flames [31], laminar burning velocities [32,33], ignition delay times [33-35], laminar premixed flames [36] and flow reactors [36,37]. The capacity of DMC to form polycyclic aromatic hydrocarbons (PAH) and soot has also been experimentally studied [38,39], showing that this oxygenated compound forms less soot than others, such as ethanol. The works involving chemical kinetic studies have shown that much of the oxygen in the DMC goes directly to CO_2, which increases the effectiveness of DMC for minimizing soot formation [e.g. 39].

Despite these laboratory studies performed with the DMC, the experimental and modeling investigations on the conversion of this oxygenated compound are still scarce, especially at high pressures, which are of interest in diesel engine applications. To our knowledge, only the works of Hu et al. [34] (up to 10 atm in shock tube) and Alexandrino et al. [35] (up to 40 atm in shock tubes and rapid compression machine) addressed experiments at high pressures. In those works, it was observed that the ignition delay time decreased with increasing pressure. It was attributed to the increase in absolute concentration of reactants at high pressures, which promotes the oxidation process. Thus, in the present work, the experimental and modeling high pressure oxidation of DMC has been studied in a large range of temperature, pressure and different stoichiometries. Specifically, the oxidation of DMC has been investigated under well-controlled flow reactor conditions in the temperature range of 500-1073 K and at pressures of 20, 40 and 60 atm. Under these conditions, the stoichiometry has been varied from fuel rich to fuel lean conditions (air excess ratios (λ) from around 0.7 to 35) by varying the concentration of oxygen

from 1470 to 73500 ppm. In this way, the concentration profile of DMC and of the main products of its oxidation (H_2, CO and CO_2) has been obtained. Moreover, the interpretation of the effect of the temperature, pressure and stoichiometry on the DMC conversion has been performed through the rate of production and sensitivity analyses, using a gas-phase detailed kinetic model previously developed by the research group. Additionally, the performance of the model used has also been evaluated through the simulation of experimental data from literature. In this sense, this work contributes to the knowledge of the combustion process of DMC and extends the experimental data available for DMC conversion.

2. Experimental methodology

The oxidation of DMC at high pressure was performed in an experimental set-up, which has been used successfully in a series of previous works of our research group (Thermochemical Process Group – GPT, University of Zaragoza), addressing high pressure gas-phase reactions [e.g. 40-43].

The reactor is a quartz tube, with an inside diameter of 6 mm and a length of 1500 mm, positioned within an AISI 316L stainless steel tube, which acts as a shell to keep pressure. This pressure shell is placed inside a three-zone electrically heated furnace with individual temperature control. The pressure inside the reactor is monitored by a differential pressure transducer (EL-PRESS Bronkhorst High-Tech) located at the reactor entrance and controlled by a pneumatic pressure valve (RCV-RC200) situated after the reactor. The maximum pressure allowed is of 80 atm. N_2 is released into the shell to avoid sudden pressure gradients inside and outside of the reactor. The maximum temperature allowed over the whole pressure range is of 1100 K. An isothermal temperature (± 5 K) throughout the 560 mm of the reaction zone is guaranteed. The surface reactions, which may occur on the surfaces of reactors, are expected to be minimized due to the use of quartz tube and high pressure [44-46].

A concentration of approximately 700 ppm of DMC is fed into the reactor using a controlled evaporator mixer (CEM), with an uncertainty of the measurements below 10%, and N_2 as a carrier gas. The amount of oxygen required to perform each oxidation experiment is calculated through the air excess ratio (λ), defined as the ratio between the inlet oxygen and the stoichiometric oxygen, according to reaction $CH_3OCOOCH_3 + 3O_2 \rightarrow 3CO_2 + 3H_2O$ (λ =1 means stoichiometric conditions; λ<1 means fuel-rich conditions; λ>1 means fuel-lean conditions). The λ values are around 0.7, 1 and 35. N_2 is used to balance the total flow rate up to 1000 mL (STP)/min. O_2 and N_2 are fed into the reactor using calibrated mass flow controllers (Bronkhorst High-Tech). All gas flow lines are heated and thermally insulated in order to prevent gas condensation.

The gas residence time in the reaction zone (τ_r) is given by Eq. 1.

$$\tau_r(\mathrm{s}) = \frac{261119 \,.\, \mathrm{P_{rz}(atm)}}{\mathrm{Q\ (mL(STP)/min)} \,.\, \mathrm{T_{rz}(K)}} \qquad \text{Eq. 1}$$

Where, Q is the total flow rate, and T_{rz} and P_{rz} are the temperature and the pressure in the reaction zone, respectively.

Downstream the reactor outlet, the system pressure is reduced to atmospheric pressure. Subsequently, the product gas stream passes through a particle filter and a condenser to be conditioned for further analysis. Finally, the concentration of DMC and products is analyzed in the product gas stream, by a micro gas chromatograph (micro-GC) (Agilent 3000A) equipped with TCD detectors. This micro-GC is calibrated to quantify DMC, CO_2, CO, H_2, ethylene, acetylene, methane, ethane, methanol, dimethyl ether and methyl formate. The uncertainty of the measurements is estimated within 5%.

The conditions for each set of experiments are summarized in Table 1, which are all performed under highly diluted conditions to minimize thermal effects due to reaction.

Table 1. Experimental conditions in the study of the oxidation of DMC at high pressures in the temperature range of 500-1073 K. N_2 is used to balance.

Set	λ	Pressure (atm)	[DMC] (ppm)	[O_2] (ppm)
1	0.64	20	759	1470
2	0.65	40	750	1470
3	0.65	60	752	1470
4	0.99	20	704	2100
5	0.96	40	732	2100
6	0.96	60	727	2100
7	31.21	20	785	73500
8	33.47	40	732	73500
9	33.20	60	738	73500

3. Modeling

The kinetic model used in the present work is the same that used in our previous investigation on the dimethoxymethane (DMM) pyrolysis [47] (the mechanism and thermodynamic data can be taken from that work).

This model includes the sub-mechanisms for different oxygenated compounds, such as DMM, methyl formate (MF) and dimethyl ether (DME), and was constructed based on the model used in the research of Alzueta et al. [37], on the oxidation of DMC at atmospheric pressure. The model of Alzueta et al. [37] is based on the GADM model [48] and its updates [e.g. 49-52], and includes the DMC oxidation sub-mechanism proposed by Glaude et al. [53], which was the first chemical kinetic sub-mechanism for DMC conversion proposed in literature, and has been widely used in several works [34,35,37]. The reaction rate constants for reactions involving DMC were obtained by Glaude et al. [53] by analogies based on the reaction rate of DME, formic acid, and methyl butanoate. The DMC submechanism includes:

1) unimolecular DMC decomposition by breaking the C-O and O-O bonds and by CO_2 elimination.

2) H-atom abstractions.

3) conversion to ether-acid (CH_3OCOOH).

4) H-atom abstraction reactions from CH_3OCOOH.

5) subsequent decomposition of the radicals formed.

Compared to the values used in the DMC oxidation sub-mechanism of Glaude et al. [53], in the model of Alexandrino et al. [47], the rate constants of two DMC specific reactions, which showed to be important in its conversion at high (reaction R1) and low (reaction R2) temperatures [35], were changed.

$CH_3OCOOCH_3$ (+M) ⇄ $CH_3OCOO + CH_3$ (+M) R1

$CH_3OCOOCH_3 + CH_3O_2 \rightleftarrows CH_3OCOOCH_2 + CH_3OOH$ R2

For reaction R1, in Alexandrino et al. [47], the rate constant estimated by Hu et al. [34], by analogy with the rate constant for the decomposition of methyl butanoate ($C_3H_5COOCH_3$) proposed by Dooley et al. [54], was used. Likewise, for reaction R2, the rate constant presented by Sun et al. [36], estimated by analogy with the reaction between methyl formate (HCO_2CH_3) and CH_3O_2 radicals proposed by Dooley et al. [55], was adopted. Table 2 shows the kinetic parameters of the reactions R1 and R2 used in the model proposed by Alexandrino et al. [47].

Table 2. Kinetic parameters of the reactions R1 and R2 used in the model employed in the present work [47].

Reaction	A	n	E_a	Reference
R1	2.55×10^{23}	-1.99	8.81×10^{4}	26
low	1.74×10^{73}	-1.60×10^{1}	8.53×10^{4}	
Troe	2.18×10^{-1} 1.00	6.38×10^{3}	8.21×10^{9}	
R2	1.13×10^{5}	2.44	16594.3	28

A in units cm^3, mol, s, and E_a in cal/mol

Troe pressure-dependent parameters are written in the following order: α, T***,T*,T**. They are required to determine the F_{cent}, and consequently the function F, to calculate the rate constant of the reaction in the fall-off region [56,57].

It is to be mentioned that Alzueta et al. [37] found that the thermodynamic data of the CH_3OCOO radical species greatly influence the calculations of the oxidation of DMC. However, reaction R1 was identified in the work of Alexandrino et al. [35] to be the cause of this event. In the work of Alexandrino et al. [47], and in the present work, reaction R1 was taken from Hu et al. [34], and no effect of thermodynamics is observed on the calculations of the oxidation of DMC.

Simulations were run with the CHEMKIN-PRO package [58]. Species thermodynamic data are required for Chemkin to calculate the reverse rate constant of reversible reactions. The thermodynamic data were taken from the same sources as the original mechanisms. The Plug Flow Reactor (PFR) model, with Fixed Gas Temperature assumption, was employed to simulate the flow reactor experiments.

4. Results and discussion

4.1. Oxidation of DMC at high pressures

The experimental data and simulations for the oxidation of 700 ppm of DMC at several pressures (20, 40 and 60 atm), under fuel-rich (λ = 0.7), stoichiometric (λ = 1), and fuel-lean conditions (λ = 35), in the 500-1073 K temperature range are shown in Fig. 1. The gas residence time (τ_r), in the reaction zone of the reactor, takes values of 4.5-10 s, 9-21 s, and 14-31 s, for pressures of 20, 40 and 60 atm, respectively, in the temperature interval considered (500-1073 K). The order of magnitude of these residence time values are similar to those used in other works [40,42,59,60].CO, CO_2 and to a lesser extent H_2, under the specific conditions considered, have been the major products detected. Only at 20 and 40 atm, under fuel-rich and stoichiometric conditions, CH_4 was detected at low concentration, less than 150 ppm (not shown). CO and CO_2 are plotted in Fig. 1 with individual Y-axis for easier reading.

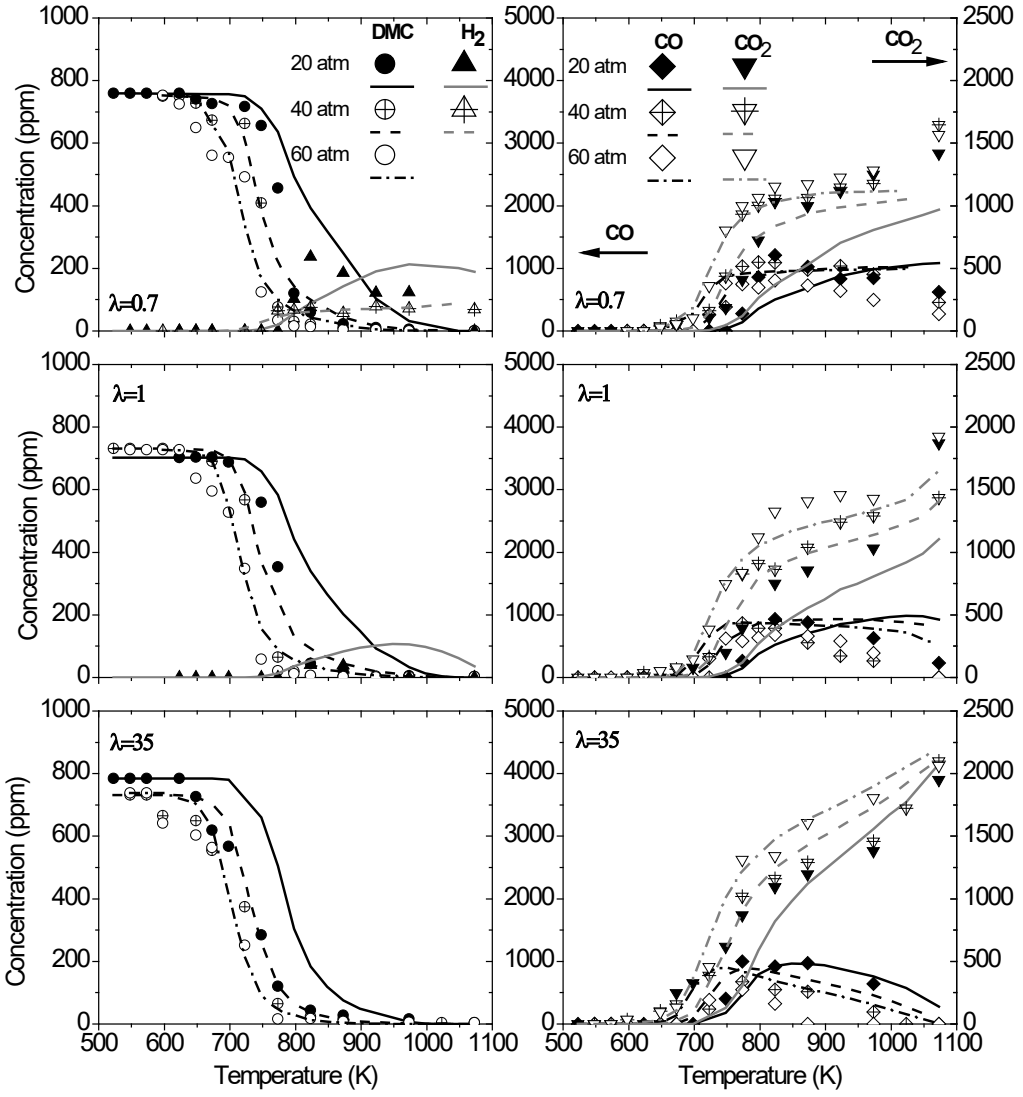

Fig. 1. Concentration profiles, as a function of temperature, of the major species found in the oxidation of DMC at pressures of 20, 40 and 60 atm, and λ = 0.7, 1 and 35 (sets 1-9 in Table 1). Experimental data (symbols), simulations (lines).

In general, the model is able to reproduce the experimental trends of the different concentration profiles, although some discrepancies are observed between experimental and simulation results. Specifically, discrepancies are observed for the CO concentration profile under fuel-rich conditions, where the model can not predict properly neither the formation nor the consumption of this species, and for CO_2 at 20 atm, where the model underpredicts its concentrations.

For a given pressure, the experimental and calculated onset temperature for DMC conversion is shifted 50 K to lower temperatures only under fuel-lean conditions, while under fuel-rich and stoichiometric conditions, the oxygen concentration does not have an apparent effect on the onset temperature of the DMC conversion. This behavior coincides with that observed in the oxidation of DMC at atmospheric pressure [37].

Fig. 2 shows a reaction pathway diagram for the oxidation of DMC obtained through a reaction rate analysis with the model used in the present work.

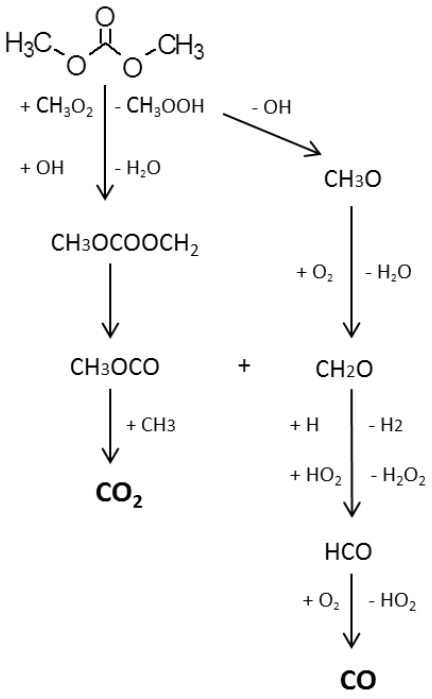

Fig. 2. Reaction pathway diagram for the conversion of DMC under high pressure conditions.

Under all the stoichiometries and pressures studied in this work, the main consumption of DMC is through the reactions with CH_3O_2 and OH radicals (reactions R2 and R3, respectively), which are promoted as oxygen concentration is increased, thus enhancing the DMC consumption under fuel-lean conditions.

$CH_3OCOOCH_3 + CH_3O_2 \rightleftarrows CH_3OCOOCH_2 + CH_3OOH$ R2

$CH_3OCOOCH_3 + OH \rightleftarrows CH_3OCOOCH_2 + H_2O$ R3

The so-called DMC radicals ($CH_3OCOOCH_2$), formed in reactions R2 and R3, further decompose to form methyl radicals and CO_2 (R4-R5 and Fig. 2). This direct formation of CO_2, instead of from oxidation of CO as usually occurs, can be observed experimentally and by model calculations in Fig. 1, where the onset of DMC consumption is accompanied by the formation of CO_2. This direct formation of CO_2 from the DMC conversion has also been observed in previous works addressing the oxidation of DMC at atmospheric and low pressure [31,36, 37,61]. Moreover, it is observed that the concentration of CO_2 increases with the increase of temperature for any stoichiometry and pressure.

$CH_3OCOOCH_2 \rightleftarrows CH_2O + CH_3OCO$ R4

$CH_3OCO \rightleftarrows CH_3 + CO_2$ R5

On the other hand, the CH_3OOH radicals formed through reaction R2 decompose to ultimately form hydroperoxyl radicals (HO_2) and CO (R6-R9 and Fig. 2). The experimental concentration profile of CO exhibits a maximum for all stoichiometries, Fig. 1, which is shifted to lower temperatures as the oxygen concentration increases.

$CH_3OOH \rightleftarrows CH_3O + OH$ R6

$CH_3O + O_2 \rightleftarrows CH_2O + HO_2$ R7

$CH_2O + H/HO_2 \rightleftarrows HCO + H_2/H_2O_2$ R8

$HCO + O_2 \rightleftarrows HO_2 + CO$ R9

It is also observed from Fig. 1 that, for a given λ value, increasing pressure shifts the start of DMC conversion to lower temperatures, with an almost negligible effect under fuel-lean conditions. Under fuel-rich and stoichiometric conditions at 20 atm, the fuel consumption starts at around 700 K. Increasing pressure to 40, and then 60 atm, the fuel starts to be consumed at 675 and 650 K, respectively. It is to be noted that, when the pressure is increased from 20 to 60 atm, the gas residence time in the reaction zone also increases (Eq. 1).

Fig. 3 evaluates individually, according to model simulations, the effect of both pressure and gas residence time on the DMC conversion, for the stoichiometric mixture (λ = 1). The individual effect of pressure (Fig. 3a) was evaluated through the use of a given gas residence time value and different pressures (60, 40 and 20 atm). According to equation 1, the residence time value was remained the same (τ_r(s) = 15667/T(K)) by changing the total gas flow rate for each pressure (Q=1000 mL (STP)/min for 60 atm, 666.66 mL (STP)/min for 40 atm and 333.33 mL (STP)/min for 20 atm). On the other hand, the individual effect of the gas residence time (Fig. 3b) was evaluated using a given pressure (60 atm) and different gas flow rates (1000 mL (STP)/min (τ_r(s) = 15667/T(K)), 1500 mL (STP)/min (τ_r(s) = 10444/T(K)) and 3001.3 mL (STP)/min (τ_r(s) = 5220/T(K))). It is observed in Fig. 3 that, as expected, both pressure and residence time influence the DMC conversion, accelerating the DMC consumption to lower temperatures as the value of these variables increases. This is on line with that observed in previous works [e.g. 43].

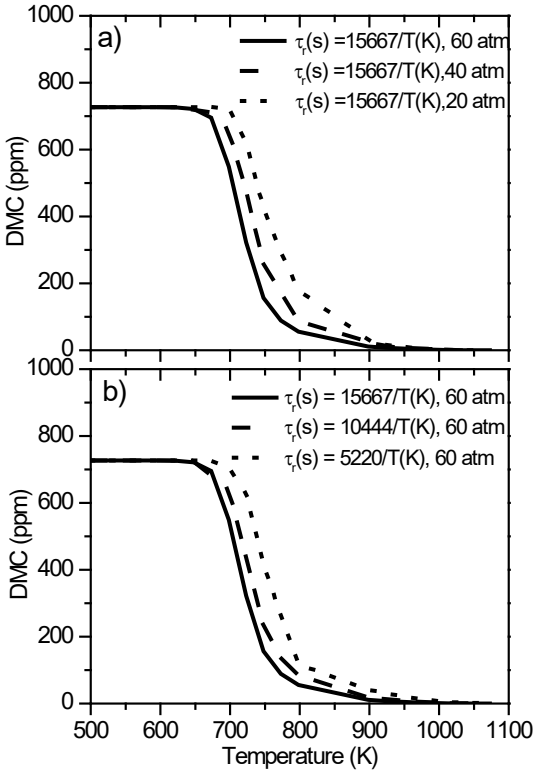

Fig. 3. Influence of the pressure (Fig. 3a) and gas residence time (Fig. 3b) on the DMC conversion for λ = 1 according to model simulations (for conditions of set 6 in Table 1).

Fig. 4 shows the results of the first-order sensitivity analysis for CO, for the different stoichiometries and pressures studied, at the temperature at which DMC starts to be consumed. For each stoichiometry, the plots of the sensitivity analysis have been made considering the top 10 reactions with the largest absolute value of the sensitivity coefficient. The sensitivity coefficients (S) are calculated as $S = A_i/Y_{CO} \times \partial Y_{CO}/\partial A_i$, where Y_{CO} is the mass fraction of CO and A_i is the pre-exponential constant for *i*th reaction [58]. Positive coefficients correspond to

reactions which promote the DMC oxidation process, while negative ones correspond to reactions which inhibit this process. It is observed that, for a given stoichiometry, the oxidation of DMC is sensitive to the same reactions for the three pressures. This could suggest that the shift in the onset of DMC conversion to lower temperatures, as pressure increases (Fig. 1), can be attributed to the increase in both the absolute concentration of reactants (DMC and O_2) and to the increase of gas residence time (Fig. 3), due to the increase in pressure, instead of a change in the controlling chemistry, as it has also been observed in the works of Hu et al. [34] and Alexandrino et al. [35].

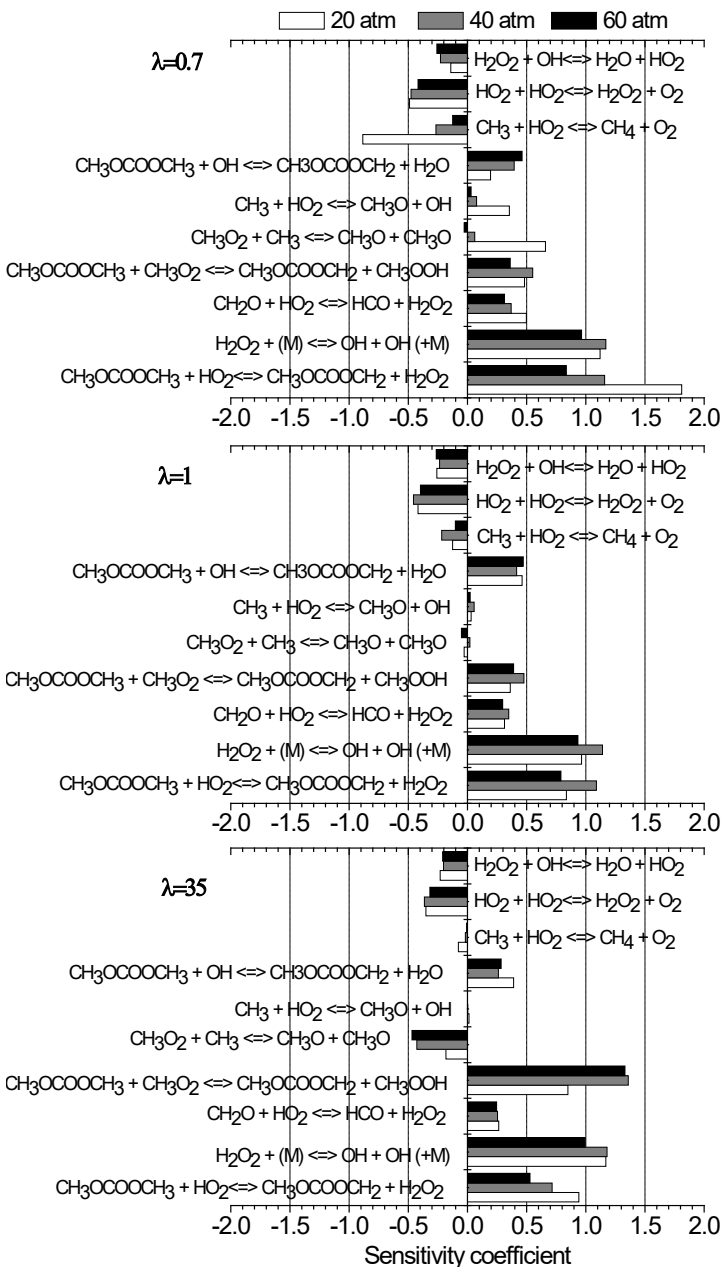

Fig. 4. First-order sensitivity analysis for CO for the high pressure (20, 40 and 60 atm) oxidation of DMC (λ = 0.7, 1 and 35) (sets 1 and 4 at 773 K, sets 2 and 5 at 723 K, sets 3, 6, and 8 at 698 K, set 7 at 748 K and set 9 at 673 K, in Table 1). Positive coefficients correspond to reactions which promote the DMC oxidation process.

As can be observed in Fig. 4, reactions R10 and R11 present positive coefficients. These reactions have been reported to be an important chain-branching sequence in many studies on the oxidation of oxygenated and hydrocarbon species at low to intermediate temperatures [62,63].

$CH_3OCOOCH_3 + HO_2 \rightleftarrows CH_3OCOOCH_2 + H_2O_2$ R10

$H_2O_2 (+M) \rightleftarrows OH + OH (+M)$ R11

They highly promote the DMC consumption, Fig. 4, because lead to the formation of two very reactive hydroxyl radicals (OH), with hydrogen peroxide (H_2O_2) as intermediate. This greatly promotes the oxidation of DMC because, as previously indicated, an important path for DMC consumption at high pressures is the H-atom abstraction from DMC by OH radicals (reaction R3), which in turn also promotes reactivity (Fig. 4).

Reactions R2 and R8 also promote the oxidation of DMC (Fig. 4). The CH_3OOH radicals produced in reaction R2 can further decompose to produce OH and CH_3O radicals (reaction R6). The latter in turn react with O_2 to finally produce OH radicals through the reaction sequence R7-R9, R12 and R11.

$CH_3OCOOCH_3 + CH_3O_2 \rightleftarrows CH_3OCOOCH_2 + CH_3OOH$ R2

$CH_3OOH \rightleftarrows OH + CH_3O$ R6

$CH_3O + O_2 \rightleftarrows CH_2O + HO_2$ R7

$CH_2O + HO_2 \rightleftarrows HCO + H_2O_2$ R8

$HCO + O_2 \rightleftarrows HO_2 + CO$ R9

$HO_2 + HO_2 \rightleftarrows H_2O_2 + O_2$ R12

$H_2O_2 (+M) \rightleftarrows OH + OH (+M)$ R11

Reaction $HO_2 + HO_2 \rightleftarrows H_2O_2 + O_2$ (R12) inhibits the oxidation of DMC (Fig. 4) because this termination reaction can compete with the promoting H-atom abstraction reaction $CH_3OCOOCH_3 + HO_2 \rightleftarrows CH_3OCOOCH_2 + H_2O_2$ (R10) reducing the OH radicals formation. If two HO_2 radicals react with each other, only two OH radicals are formed (reaction R12 followed by reaction R11), while if two HO_2 radicals react with DMC, two H_2O_2 molecules could be formed (through reaction R10), ultimately leading to the formation of four OH radicals (through reaction R11), thereby promoting the oxidation.

The reaction of CH_3O_2 radicals with methyl radicals to produce two CH_3O radicals, R13, becomes an inhibiting reaction as λ increases, Fig. 4, because it competes with the promoting reaction $CH_3OCOOCH_3 + CH_3O_2 \rightleftarrows CH_3OCOOCH_2 + CH_3OOH$ (R2) which sensitivity coefficients, for all the pressures, are higher under fuel-lean conditions than under fuel-rich and stoichiometric conditions.

$CH_3O_2 + CH_3 \rightleftarrows CH_3O + CH_3O$ R13

According to model calculations, the CH_3O_2 radicals are mainly formed by the reaction of O_2 with methyl radicals (Reaction R14).

403 $CH_3 + O_2$ (+M) ⇄ CH_3O_2 (+M) R14

404

405 Consequently, the enhancement in the sensitivity coefficient of reaction R2 under fuel-lean
406 conditions, could explain the early DMC consumption when compared with fuel-rich and
407 stoichiometric conditions for a given pressure (Fig. 1). A higher oxygen concentration in the
408 reactant mixture increases the formation of the CH_3O_2 radicals and, consequently, favours the
409 DMC consumption through the promoting reaction R2.

410

411 ~~It is worth to mention that~~ In order to try to improve the fitting between the mechanism and
412 experimental results, the reaction rates of the most influencing reactions found in the sensitivity
413 analysis (Fig. 4) were varied and the results obtained were analyzed. However, no
414 significantimprovements were observed compared to what is observed in Fig. 1. Anyway, as
415 seen in the sentivity analysis of Fig. 4, reactions R3 and R10 appear to be those that affect more
416 both the concentration of CO and the concentration of CH_3Ot. In this sense, further re-
417 evaluation of the kinetic parameters of reactions R3 and R10 would be of interest.

418

419 In order to evaluate the capacity of the model used in the present work to predict the
420 experimental data at atmospheric pressure, Fig. 5 plots the experimental and modeling results
421 for DMC conversion, and formation of CO and CO_2, in the oxidation of DMC at atmospheric
422 pressure, for λ = 0.3, 0.7, 1 and 35. The experimental data were obtained by Alzueta et al. [37]
423 in a tubular flow reactor operating at 800-1400 K, with approximately 300 ppm of DMC and using
424 N_2 to balance. The gas residence time is a function of temperature, τ_r (s) = 195/T(K). Simulation
425 results obtained with the model used in Alzueta et al. [37] and the one used in the present work
426 are presented. As it is observed, the model proposed by Alexandrino et al. [47] simulates very
427 well the oxidation of DMC at atmospheric pressure, with a better performance than the model
428 of Alzueta et al. [37], mainly under fuel-rich and stoichiometric conditions. The improvement in

the simulations using the model of Alexandrino et al. [47], with respect to the simulations using the model of Alzueta et al. [37], is mainly due to the adoption of the rate constant, from Hu et al. [34], of the very important reaction $CH_3OCOOCH_3$ (+M) ⇄ $CH_3OCOO + CH_3$ (R1), that promotes DMC conversion at high temperatures, as it was previously indicated.

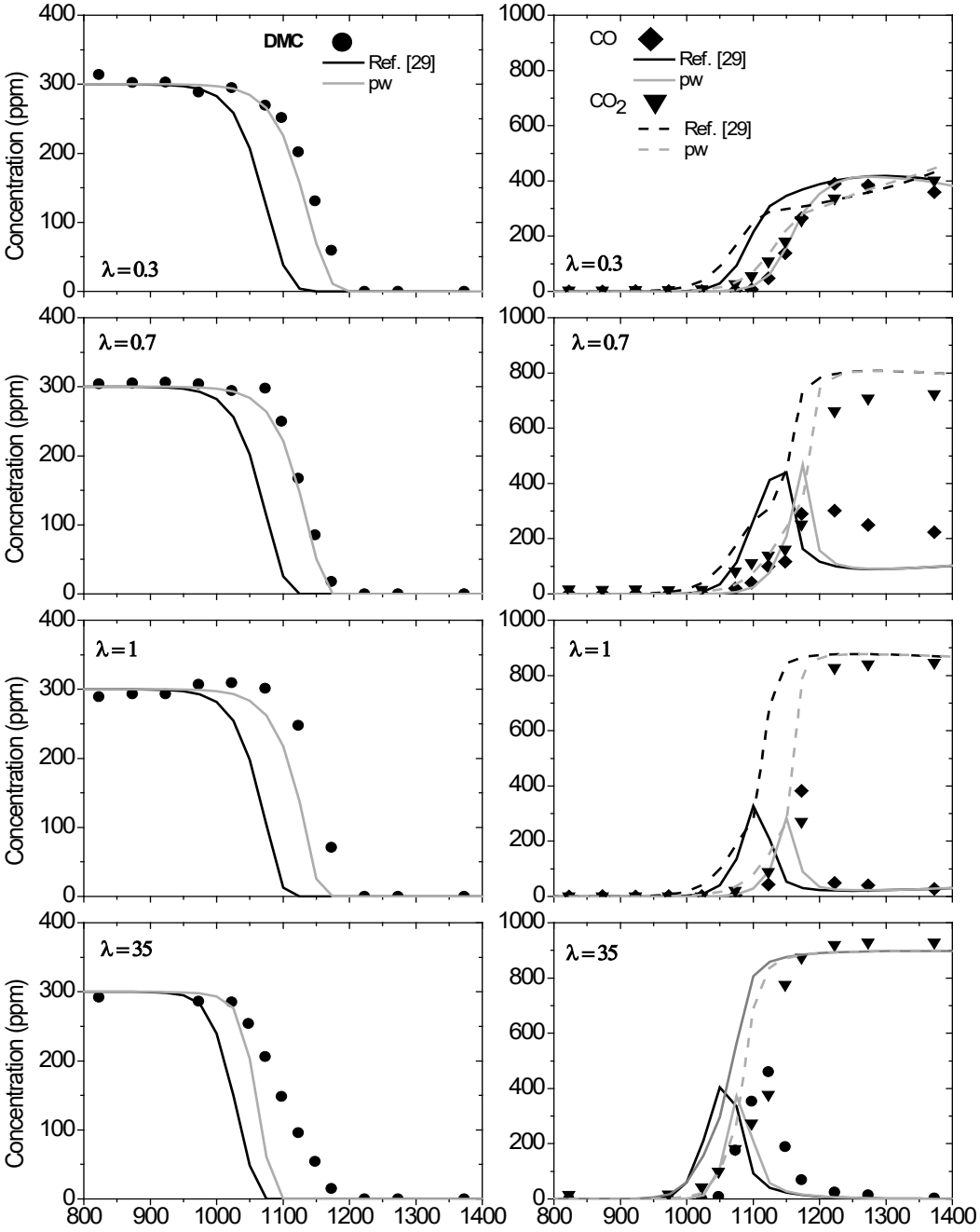

Fig. 5. Comparison between the simulation of the oxidation of DMC at atmospheric pressure [37], for λ = 0.3, 0.7, 1, and 35, using the model from Alzueta et al. [37] and the model proposed by Alexandrino et al. [47] (pw).

Additionally, the performance of the model used in the present work was also evaluated through the simulation of the experimental data of ignition delay times of DMC from the work of Alexandrino et al. [35], obtained using low and high pressure shock tubes and a rapid compression machine. The experiments cover the temperature range of 795-1585 K, DMC concentration of 0.75% and 1.75%, pressures of 2, 20, and 40 atm, and λ= 0.5, 1, and 2. It is observed in Fig. 6 that the model of Alexandrino et al. [47] fits well the experimental data, and the simulation data are very similar to those obtained using the model proposed in Alexandrino et al. [35].

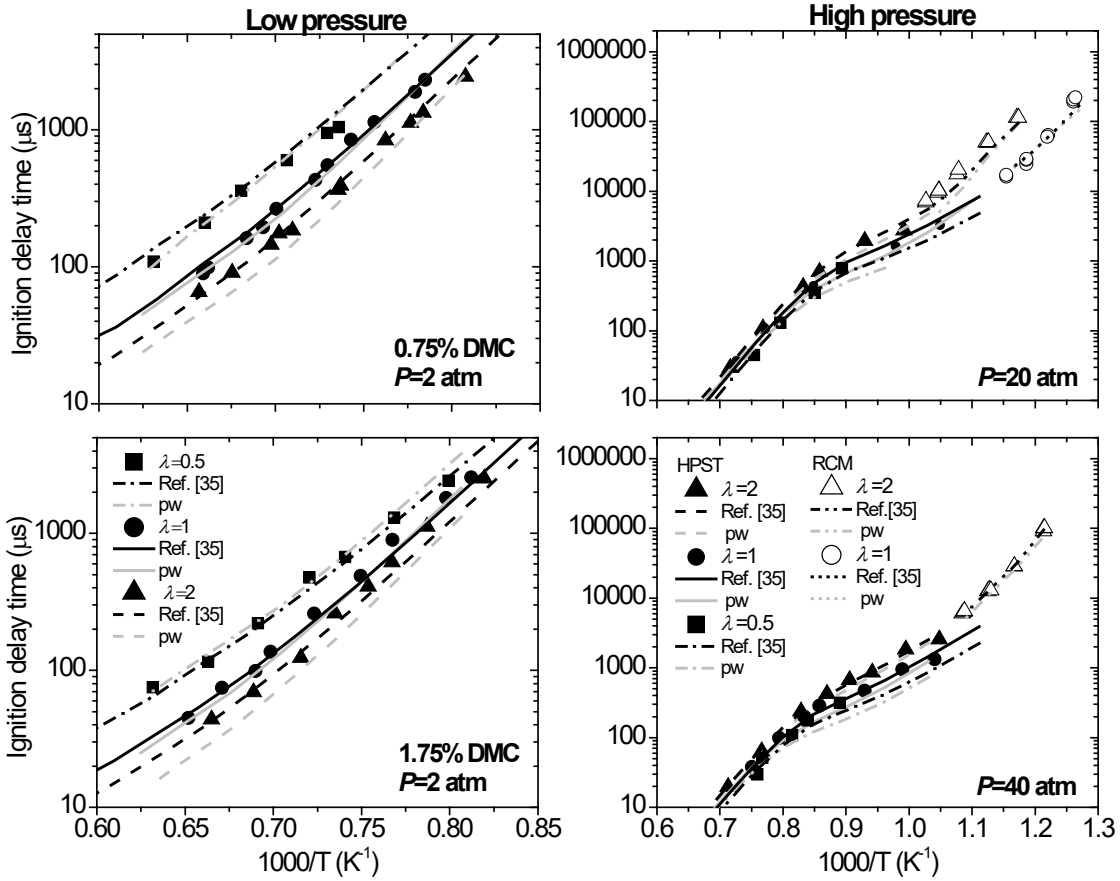

Fig. 6**.** Experimental data (symbols) of the ignition delay times of DMC [35] in a low pressure shock tube (left) and in a high pressure shock tube and rapid compression machine (right) together with simulations (lines) using the model from Alexandrino et al. [35] and the model proposed by Alexandrino et al. [47] (pw).

5. Conclusions

This work includes the experimental and modeling study of the oxidation of DMC at high pressures, in a flow reactor operating at 20, 40, and 60 atm, in the temperature range of 500-1073 K, and under fuel-rich (λ = 0.7), stoichiometric (λ = 1), and fuel-lean conditions (λ = 35). The performance of the model was also evaluated with data from literature (flow reactor at atmospheric pressure and ignition delay times at low and high pressures).

Experimental data and simulations show that, for a given pressure, the onset of DMC consumption is shifted to lower temperatures only under fuel-lean conditions, while under fuel-rich and stoichiometric conditions there is not a noticeable effect of the stoichiometry on the onset temperature of DMC consumption. The effect of the fuel-lean condition on the onset temperature of the oxidation of DMC can be attributed to a higher formation of CH_3O_2 radicals, whose reaction with DMC has a high promoting effect on the oxidation of DMC under this stoichiometry condition. Regarding the effect of pressure on the fuel conversion, increasing pressure shifts the onset of fuel conversion to lower temperatures with an almost negligible effect under fuel-lean conditions. Such shift was due to effects of both the increase of the absolute concentration of reactants and to the increase of gas residence time, due to the increase in pressure, instead of a change in the controlling chemistry. Regarding the performance of the model used, it can be concluded that it predicts reasonably well the oxidation of DMC at both atmospheric and high pressures, in a wide range of stoichiometries, temperatures and gas residence times, using different experimental set-ups. However, despite the fact that this model captures the tendency of the experimental data, some discrepancies between experimental and model results are found for CO under rich-fuel conditions and for CO_2 at 20 atm, and further improvement is needed to get a better accuracy.. It is not clear at present what are the main issues to be considered for improvement of the mechanism predictions. Possibilities would include the calculation and incorporation of pressure-dependent rate constants in the DMC oxidation sub-mechanism reactions (mainly in reactions R3 and R10), a more precise determination of the most sensitive reactions, etc.

Acknowledgement

The authors acknowledge the financial support from the Aragón Government (Ref. T22_20R), co-funded by FEDER 2014-2020 "*Construyendo Europa desde Aragón*", and MINECO, MCIU and

FEDER (Projects CTQ2015-65226 and RTI2018-098856-B-I00). Ms. K. Alexandrino acknowledges to MINECO the pre-doctoral grant awarded (BES-2013-063049).

Competing interests

Authors have no competing interests to declare

References

[1] Liotta FJ, Montalvo DM. The effect of oxygenated fuels on emissions from a modern heavy-duty diesel engine. SAE Technical Paper 932734, 1993.

[2] Patil AR, Taji, SG. Effect of oxygenated fuel additive on diesel engine performance and emission: a review. J Mech Civil Eng 2013;30–35.

[3] Chen G, Shen Y, Zhang Q, Yao M, Zheng Z, Liu H. Experimental study on combustion and emission characteristics of a diesel engine fueled with 2,5-dimethylfuran–diesel, n-butanol–diesel and gasoline–diesel blends. Energy 2013;54:333–342.

[4] Pan M, Zheng Z, Huang R, Zhou X, Huang H, Pan J, Chen Z. Reduction in PM and NOx of a diesel engine integrated with n-octanol fuel addition and exhaust gas recirculation. Energy 2019;187: 115946.

[5] Duan X, Xu Z, Sun X, Deng B, Liu J. Effects of injection timing and EGR on combustion and emissions characteristics of the diesel engine fuelled with acetone–butanol–ethanol/diesel blend fuels. Energy 2021;231: 121069.

[6] Turner D, Xu H, Cracknell, RF, Natarajanc V, Chen X. Combustion performance of bio-ethanol at various blend ratios in a gasoline direct Injection engine. Fuel 2011;90:1999−2006.

[7] Chen H, Shuai S J, Wang J X. Study on combustion characteristics and PM emission of diesel engines using ester − ethanol −diesel blended fuels. Proc. Combust. Inst. 2007;31:2981−2989.

534 [8] Sukjit E, Herreros J M, Dearn K D, García-Contreras R, Tsolakis A. The effect of the addition of
535 individual methyl esters on the combustion and emissions of ethanol and butanol-diesel blends.
536 Energy 2012;42:364−374.
537 [9] Taghizadeh-Alisaraei A, Rezaei-Asl A. The effect of added ethanol to diesel fuel on
538 performance, vibration, combustion and knocking of a CI engine. Fuel 2016:185;718 − 733.
539 [10] Esarte C, Callejas A, Millera Á, Bilbao R, Alzueta MU. Influence of the concentration of
540 ethanol and the interaction of compounds in the pyrolysis of acetylene and ethanol mixtures.
541 Fuel 2011;90:844–849.
542 [11] Demirbas A. Competitive liquid biofuels from biomass. Appl. Energy 2011;88:17–28.
543 [12] Cheung CS, Lee SC, Kwok A, Tung CW. Effect of dimethyl carbonate blended diesel on
544 emissions of a 4-cylinder diesel engine. HKIE Transactions 2005;12:15-20.
545 [13] Zhang GD, Liu H, Xia XX, Zhang WG, Fang JH. Effects of dimethyl carbonate fuel additive on
546 diesel engine performances. Proc Inst Mech Eng D 2005;219:897.
547 [14] Miyamoto N, Ogawa H, Arima T. Improvement of diesel combustion and emissions with
548 addition of various oxygenated agents to diesel fuels. SAE Technical Paper 962115,2014.
549 [15] Yang J, Jiang Y, Karavalakis G, Johnson KC, Kumar S, Cocker DR, Durbin TD. Impacts of
550 dimethyl carbonate blends on gaseous and particulate emissions from a heavy-duty diesel
551 engine. Fuel 2016;184:681–688.
552 [16] Rounce P, Tsolakis A, Leung P, York APE. A Comparison of diesel and biodiesel emissions
553 using dimethyl carbonate as an oxygenated additive. Energy Fuels 2010;24:4812–4819.
554 [17] Cheung CS, Liu MA, Lee SC, Pan KY. Experimental study on emission characteristics of diesel
555 engines with diesel fuel blended with dimethyl carbonate. Clean Air 2005;6:239–253.
556 [18] Cheung CS, Zhu R, Huang Z. Investigation on the gaseous and particulate emissions of a
557 compression ignition engine fueled with diesel–dimethyl carbonate blends. Sci Total Environ
558 2011;409:523–529.

559 [19] Pan M, Qian W, Zheng Z, Huang R, Zhou X, Huang H, Li M. The potential of dimethyl
560 carbonate (DMC) as an alternative fuel for compression ignition engines with different EGR
561 rates. Fuel 2019;257:115920
562 [20] Wei J, Lu W, Pan M, Liu Y, Cheng X, Wang C. Physical properties of exhaust soot from
563 dimethyl carbonate-diesel blends: Characterizations and impact on soot oxidation behavior.
564 Fuel 2020;279:118441.
565 [21] Sun W, Yang B, Hansen N, Moshammer K. The influence of dimethoxy methane
566 (DMM)/dimethyl carbonate (DMC) addition on a premixed ethane/oxygen/argon flame. Proc
567 Combust Inst 2017;36: 449-457.
568 [22] Paladpokkrong C, Liu D, Ying Y, Wang W, Zhang R. Soot reduction by addition of dimethyl
569 carbonate in normal and inverse ethylene diffusion flames: Nanostructural evidence. J Environ
570 Sci 2018;72:107-117.
571 [23] Poungsombate A, Imyen T, Dittanet P, Embley B, Kongkachuichay P. Direct synthesis of
572 dimethyl carbonate from CO2 and methanol by supported bimetallic Cu–Ni/ZIF-8 MOFcatalysts.
573 J Taiwan Inst Chem Eng 2017;80:16–24.
574 [24] Tan HZ, Wang ZQ, Xu ZN, Sun J, Xu YP, Chen QS, Chen Y, Guo GC. Review on the synthesis
575 of dimethyl carbonate. Catal Today 2018;316:2-12
576 [25] Kumar P, Srivastava VC, Štangar UL, Mušič B, Mishra IM, Meng Y. Recent progress in
577 dimethyl carbonate synthesis using different feedstock and techniques in the presence of
578 heterogeneous catalysts. Catal Rev 2019, DOI: 10.1080/01614940.2019.1696609.
579 [26] Vertin KD, Ohi JM, Naegeli DW. Methylal and methylal–diesel blended fuels for use in
580 compression-ignition engines. SAE paper 1999-01-1508, 1999.
581 [27] Wijnen, MHJ. Decomposition of dimethyl carbonate on quartz. J Chem Phys 1961;34:465.
582 [28] Thynne, JCJ, Gray, P. The methyl-radical-sensitized decomposition of gaseous dimethyl
583 carbonate. Trans Faraday Soc 1962;58:2403–2409.

584 [29] Yee MJ, Thynne JCJ. Photolysis of dimethyl carbonate. Trans Faraday Soc 1966;62:3154–
585 3161.
586 [30] Cross JTD, Hunter R, Stimson, R. The thermal decomposition of simple carbonate esters.
587 Aust J Chem 1976;29:1477–1481.
588 [31] Sinha A, Thomson MJ. The chemical structures of opposed flow diffusion flames of C3
589 oxygenated hydrocarbons (isopropanol, dimethoxy methane, and dimethyl carbonate) and their
590 mixtures. Combust Flame 2004;136:548–556.
591 [32] Bardin ME, Ivanov EV, Nilsson EJK, Vinokurov VA, Konnov AA. Laminar burning velocities of
592 dimethyl carbonate with air. Energy Fuels 2013;27:5513–5517.
593 [33] Atherley T, de Persis S, Chaumeix N, Fernandes Y, Bry A, Comandini A, Mathieu O, Alturaifi
594 S, Mulvihill CR, Petersen EL. Laminar flame speed and shock-tube multi-species laser absorption
595 measurements of Dimethyl Carbonate oxidation and pyrolysis near 1 atm. Proc Combust Inst
596 2021:38: 977–985.
597 [34] Hu E, Chen Y, Zhang Z, Pan L, Li Q, Cheng Y, Huang Z. Experimental and kinetic study on
598 ignition delay times of dimethyl carbonate at high temperature. Fuel 2015;140:626–632.
599 [35] Alexandrino K, Alzueta MU, Curran HJ. An experimental and modeling study of the ignition
600 of dimethyl carbonate in shock tubes and rapid compression machine. Combust Flame
601 2018;188:212–226.
602 [36] Sun W, Yang B, Hansen N, Westbrook CK, Zhang F, Wang G, Moshammer K, Law CK (2016).
603 An experimental and kinetic modeling study on dimethyl carbonate (DMC) pyrolysis and
604 combustion. Combust Flame 2016;164:224–238.
605 [37] Alzueta MU, Salinas P, Millera Á, Bilbao R, Abián M. A study of dimethyl carbonate
606 conversion and its impact to minimize soot and NO emissions. Proc Combust Inst 2017;36:3985–
607 3993.
608 [38] Viteri F, Salinas J, Millera Á, Bilbao R, Alzueta MU. Pyrolysis of dimethyl carbonate: PAH
609 formation. J Anal Appl Pyrol 2016;122:524–530.

610 [39] Alexandrino K, Salinas J, Millera Á, Bilbao R, Alzueta MU. Sooting propensity of dimethyl
611 carbonate, soot reactivity and characterization. Fuel 2016;183:64–72.
612 [40] Colom-Díaz JM, Millera Á, Bilbao R, Alzueta AM. High pressure study of H_2 oxidation and its
613 interaction with NO. Int. J. Hydrog. Energy 2019;44:6325-6332.
614 [41] Colom-Díaz JM, Abián M, Millera Á, Bilbao R, Alzueta MU. Influence of pressure on H_2S
615 oxidation. Experiments and kinetic modeling. Fuel 2019;258:116145.
616 [42] Marrodán L, Millera Á, Bilbao R, Alzueta MU. High-pressure study of methyl formate
617 oxidation and its interaction with NO. Energy Fuels 2014;28:6107–6115.
618 [43] Marrodán L, Royo E, Millera Á, Bilbao R, Alzueta MU. High pressure oxidation of
619 dimethoxymethane. Energy Fuels 2015;29:3507–3517.
620 [44] Hashemi H, Christensen JM, Glarborg P. High-pressure pyrolysis and oxidation of ethanol.
621 Fuel 2018; 218:247–257.
622 [45] Hashemi H, Christensen JM, Gersen S, Glarborg P. Hydrogen oxidation at high pressure and
623 intermediate temperatures: Experiments and kinetic modeling. Proc Combust Inst 2015;
624 35:553–560.
625 [46] Hashemi H, Christensen JM, Gersen S, Levinsky H, Klippenstein SJ, Glarborg P. High-pressure
626 oxidation of methane . Combust Flame 2016; 172:349–364.
627 [47] Alexandrino K, Millera Á, Bilbao R, Alzueta MU. Gas and soot formed in the
628 dimethoxymethane pyrolysis. Soot characterization. Fuel Process Technol 2018;179:369–377.
629 [48] Glarborg P, Alzueta MU, Dam-Johansen K, Miller JA. Kinetic modeling of hydrocarbon/nitric
630 oxide interactions in a flow reactor. Combust Flame 1998;115:1–27.
631 [49] Abián M, Esarte C, Millera Á, Bilbao R, Alzueta MU. Oxidation of acetylene-ethanol mixtures
632 and their interaction with NO. Energy Fuels 2008;22:3814–3823.
633 [50] Abián M, Giménez-López, J, Bilbao R, Alzueta MU. Effect of different concentration levels of
634 CO2 and H2O on the oxidation of CO: Experiments and modeling. Proc Combust Inst
635 2011;33:317–323.

636 [51] Alzueta MU, Borruey M, Callejas A, Millera Á, Bilbao R. An experimental and modeling study
637 of the oxidation of acetylene in a flow reactor. Combust Flame 2008;152:377–386.
638 [52] Glarborg P, Østberg M, Alzueta MU, Dam-Johansen K, Miller JA. The recombination of
639 hydrogen atoms with nitric oxide at high temperatures. Proc Combust Inst 1999;27:219–227.
640 [53] Glaude PA, Pitz WJ, Thomson MJ. Chemical kinetic modeling of dimethyl carbonate in an
641 opposed-flow diffusion flame. Proc Combust Inst 2005;30:1111–1118.
642 [54] Dooley S, Curran HJ, Simmie JM. Autoignition measurements and validated kinetic model
643 for the biodiesel surrogate, methyl butanoate. Combust Flame 2008;153:2–32.
644 [55] Dooley S, Burke MP, Chaos M, Stein Y, Dryer FL, Zhukov VP, Finch O, Simmie JM, Curran HJ.
645 Methylformate oxidation: speciation data, laminar burning velocities, ignition delay times, and
646 validated chemical kinetic model. Int J Chem Kinet 2010;42:527–549.
647 [56] CHEMKIN Release 4.0, Theory Manual, Reaction Design, Inc., San Diego, CA (2004).
648 [57] Golden DM, Barker JR. Pressure- and temperature-dependent combustion reactions.
649 Combust Flame 2011;158: 602–617.
650 [58] CHEMKIN-PRO 15131, Reaction Design, San Diego (2013).
651 [59] Hashemi H, Christensen JM, Marshall P, Glarborg P. Acetaldehyde oxidation at elevated
652 pressure. Proc Combust Inst 2021;38:269-278.
653 [60] Kaczmarek D, Herzler J, Porras S, Shaqiri S, Fikri M, Schulz C, Atakan B, Maas U, Kasper T.
654 Plug-flow reactor and shock-tube study of the oxidation of very fuel-rich natural gas/DME/O2
655 mixtures. Combust Flame 2021;225:86-103.
656 [61] Chen G, Yu W, Fu J, Mo J, Huang Z, Yang J, Wang Z, Jin H, Qi, F. Experimental and modeling
657 study of the effects of adding oxygenated fuels to premixed n-heptane flames. Combust Flame
658 2012;159:2324–2335.
659 [62] Herbinet O, Battin-Leclerc. Progress in understanding low-temperature organic compounds
660 oxidation using a jet-stirred reactor. Int J Chem Kinet 2014;46:619–639.

661 [63] Pitz WJ, Westbrook CK. Chemical kinetics of the high pressure oxidation of n-butane and its
662 relation to engine knock. Combust Flame 1986;63:113–133.